

Pyribole structure types

J. E. CHISHOLM

Mineralogy Department, British Museum (Natural History), Cromwell Road, London, SW7 5BD

ABSTRACT. A set of pyribole structures can be derived from a model *I*-beam containing two distinct silicate chains in which the tetrahedra are rotated by different amounts. The model allows some tetrahedral distortion and is not bound by the parity rule (Thompson, 1970). A subset of pyribole structures which includes all the commonly occurring types can be defined using a new rule: that the structure may contain two types of tetrahedral layer, but no tetrahedral layer may contain two types of tetrahedral chain. This rule is more fundamental than the parity rule and has its origin in the optimization of the edge-to-edge packing of the tetrahedral chains into layers. *Pnm*₂ (amphibole) and *Pbc*₂ (pyroxene) emerge as space groups for 'low protopyriboles'. The approach used here leads naturally to the - and ×-chains notation of Thompson used by Veblen and Burnham (1978).

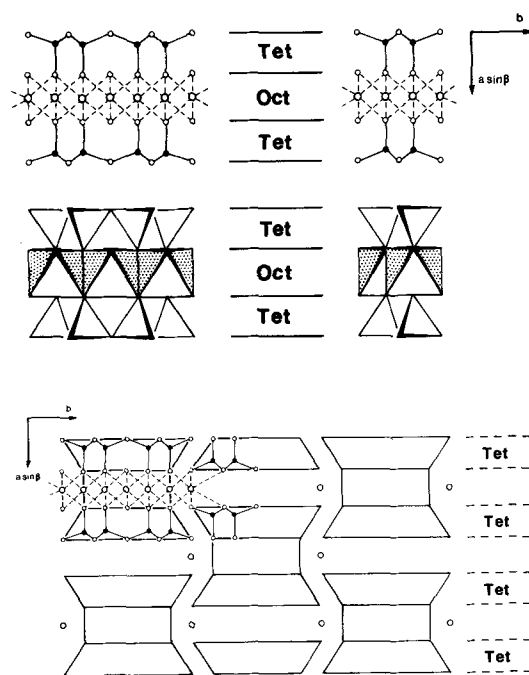
In 1970, J. B. Thompson drew attention to the relationships among the crystal structures of the pyroxenes, the amphiboles and the micas (including talc) and revived the term 'biopyribole' to describe this 'polysomatic series' (Thompson, 1978). Possible geometrical arrangements for the structures of pyroxenes and amphiboles (the 'pyriboles') were also considered by Thompson (1970) and the applicability of his ideas to the real structures of amphiboles (Papike and Ross, 1970) and pyroxenes (Papike *et al.*, 1973) was soon explored.

The pyribole structures are all composed of building units usually called '*I*-beams' (Papike and Ross, 1970) which consist of a strip of cation octahedra $\parallel c$ sandwiched between two chains of SiO₄ tetrahedra (fig. 1). The combination of the octahedral strip and two silicate double chains in the amphibole *I*-beam has a mirror plane $\perp b$ which appears in the space group. The two single silicate chains in the pyroxene *I*-beam combined with the narrower octahedral strip give a *c*-glide $\perp b$ in that case, as do the triple silicate chains and wider octahedral strip in jimthompsonite (Veblen and Burnham, 1978). The amphibole structure is used here to illustrate the derivation of possible structure types but similar arguments apply to the pyroxenes and jimthompsonite.

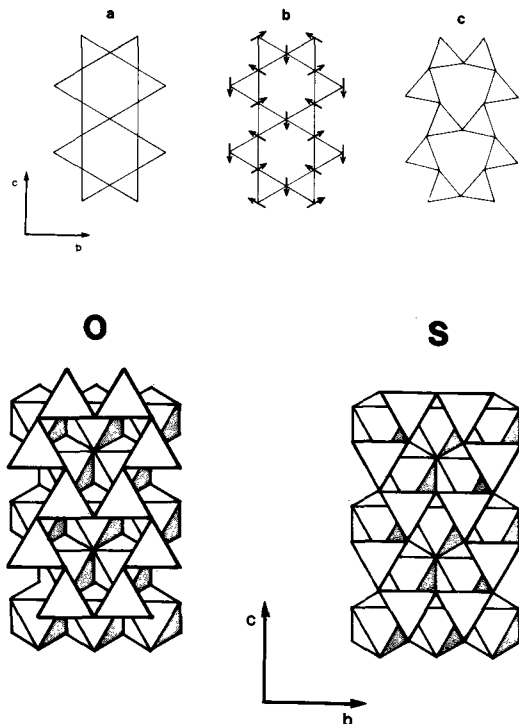
The packing of the *I*-beams in pyribole structures is shown schematically for amphibole in fig. 2. The

chains of tetrahedra are packed edge to edge in layers $\parallel (100)$, with the apices of tetrahedra in alternate double chains in amphiboles, alternate single chains in pyroxenes, pointing in opposite directions along the normal to (100) (i.e. *a* or *a* sin β).

An idealized version of the double chain of SiO₄ tetrahedra in the amphibole structure is shown in fig. 3(a). In the 'fully extended chain', the six-membered rings of tetrahedra are perfectly hexagonal. In real amphibole structures, tetrahedra



FIGS. 1 and 2. FIG. 1 (above). The '*I*-beam' building units of the amphibole (left) and pyroxene (right) structures are made up of a strip of MO₆ octahedra (labelled Oct) sandwiched between chains of SiO₄ tetrahedra (Tet). FIG. 2 (below). The *I*-beams pack together to form the amphibole structure in such a way that the tetrahedra lie in layers $\parallel (100)$ (marked Tet) with tetrahedra in alternate chains pointing along $+a \sin \beta$ and $-a \sin \beta$.



FIGS. 3 and 4. FIG. 3 (*above*). (a) Idealized fully extended double chain in amphibole in which the rings of six tetrahedra are perfectly hexagonal. Rotation of the tetrahedra about $a \sin \beta$ in the directions shown by the arrows in (b) leads to the partially rotated chain (c) in which the symmetry of the six-membered rings of tetrahedra is reduced to trigonal. FIG. 4 (*below*). Rotation of the tetrahedra in the chains can occur in two senses relative to the adjacent octahedral strip: *O*-rotation when the triangular bases of the tetrahedra point in the Opposite direction along c to the nearest triangular faces of the octahedral strip; *S*-rotation when the basal triangles of the tetrahedra and the nearest octahedron faces point in the Same direction along c . *O*- and *S*-rotations are shown for completely rotated tetrahedra when the six-membered rings of tetrahedra form triangles. Partial rotations may occur in either of the senses *O* or *S*.

are rotated about the normal to (100) as in fig. 3(b), and the symmetry of the six-membered ring is reduced to trigonal (fig. 3(c)). Distortions of a similar kind occur in the single tetrahedral chains of the pyroxene structure.

Thompson (1970) proposed a model for the pyribole structure types which took into account the possibility of tetrahedral rotation. If the rotations are completed so that the six-membered ring of tetrahedra forms a triangle (fig. 4), it becomes clear that the rotation of the tetrahedra may occur in two senses relative to the adjacent octahedral

strip. The triangular tetrahedron faces normal to $a \sin \beta$ may be in the same orientation as the nearest triangular faces of the octahedral strip (*S*-rotation, fig. 4) or oppositely orientated, i.e. with their corners 'pointing' in opposite directions (*O*-rotation, fig. 4). Partial rotations of the tetrahedra may occur in either of these two senses.

The direction of the octahedral strip must also be defined. Following Papike and Ross (1970), it is taken to be positive (+) if the lower triangular faces of the octahedra viewed towards $-a^*$ have one corner pointing in the $+c$ direction. If the lower faces have one corner pointing in the $-c$ direction, the strip direction is said to be negative (-). As Law and Whittaker (1980) have pointed out, the octahedral strip direction has no absolute meaning as its definition depends on the choice of the $+c$ crystallographic axis. However, the relative directions of the octahedral strips need to be considered in deriving possible *I*-beam arrangements, in which the octahedral strip directions may differ.

Thompson (1970) shows that the edge-to-edge packing of chains of rotated tetrahedra into layers $\parallel (100)$ should in principle limit the possible combinations of partial *O*- and *S*-rotations and octahedral strip directions. The constraint imposed is expressed in the 'parity rule': where the tetrahedral layer lies between similarly directed octahedral strips, the tetrahedra in the two chains must be rotated in the same sense. A tetrahedral layer between oppositely directed octahedral strips must have alternate chains rotated in opposite senses. The set of model pyribole structures derived by Thompson (1970) is based on this 'parity rule'. Following this rule, two types of tetrahedral chain have been defined: $-$ chains, lying in layers between similarly directed octahedral strips, and \times -chains, lying in layers between oppositely directed octahedral strips (Veblen and Burnham, 1978).

The complete *O*- and *S*-rotations shown in fig. 4 bring the oxygen atoms into cubic and hexagonal close-packed arrays (Thompson, 1970; Papike *et al.*, 1973). Law and Whittaker (1980) have derived a set of model pyribole structures from the possible sequences of close-packed oxygen planes. Using this approach, the 'parity rule' emerges as an inevitable consequence of the stacking of close-packed planes. The limitations of a close-packed model and the atomic arrangements predicted by it are discussed by Law and Whittaker.

A further model for the pyroxene structures has been proposed by Pannhorst (1979), which uses a different notation allowing for both extended and rotated chains.

The model structures so far derived have shed

much useful light on the tetrahedral chain distortions and the cation coordination in real pyriboles. However, the models have two major drawbacks: they predict many possible structural arrangements which are not found in nature, and at the same time fail to include arrangements (notably ortho- and proto-pyribole) which do exist.

These difficulties arise essentially because chains of fully or partially rotated tetrahedra do not satisfactorily represent the real pyribole structural units, in which the distortion of the tetrahedra themselves can play an important role.

As pointed out by Law and Whittaker (1980), the models all assume that the structure type is controlled by the stacking of layers along a or $a \sin \beta$. The key factor controlling the structure type is actually the lateral linking of the I -beams along the b axis via the $M4$ (amphibole) or $M2$ (pyroxene) cations (Whittaker, 1960*a, b*).

This paper presents a structural model for the pyriboles which is closer to the real structures. The model allows for some distortion of the tetrahedra and the constraints imposed by layer stacking along a or $a \sin \beta$ are removed. The set of polytypes predicted is directly related to those which actually occur. The derivation also helps to clarify the factors controlling the atomic packing and shed some light on the phase transformations between the pyribole structure types.

Structural model for an I-beam. As in previous models, the I -beams (fig. 1) are assumed to have along their centre line an idealized strip of octahedra sharing edges and containing the $M1$ cations in pyroxene and the $M3$, $M1$, and $M2$ cations in amphibole. For the $M2$ sites in pyroxene and the $M4$ in amphibole, no assumptions are made, though of course these cations must have a reasonable coordination polyhedron if a structure is to be capable of existence. The model thus permits some change in the polyhedra at the edges of the I -beam.

The direction of the octahedral strip is defined in the same way as in previous work (see above).

The tetrahedra in each of the two chains in the I -beam are assumed to be partially O - or S -rotated; the actual sense of rotation in each chain is unspecified. The two chains are assumed to have different partial rotations and the letters P and Q are introduced to denote these in order to emphasize that the sense of the rotations is unspecified and that the rotations are partial (Law and Whittaker (1980) use O and S for complete rotations). The P and Q notation should not be confused with Thompson's (1978) use of P and M for pyroxene and mica slabs, nor with the use of P and N by Sueno *et al.* (1976) to describe differences in $M2$ coordination in pyroxene.

An I -beam can be denoted $P+Q$ but can take up other orientations $P-Q$, $Q+P$, $Q-P$, according to the direction of the octahedral strip and the sequence of the two types of tetrahedral chain along $a \sin \beta$ (fig. 5).

The effect of symmetry operations on an I -beam with partially rotated tetrahedral chains can be derived in the same way as for fully rotated chains (Law and Whittaker, 1980). No symmetry operation will alter the sense (O - or S -) or the magnitude of the tetrahedral rotations P and Q . Such an operation may, however, alter the sequence of the two kinds of tetrahedral chain P and Q along the direction $a \sin \beta$ and/or reverse the octahedral strip direction. Thus starting from $P+Q$, 180° rotation about $a \sin \beta$ reverses the octahedral strip direction but does not affect the sequence of tetrahedral strips and gives $P-Q$ (Table I). Reflection in a plane perpendicular to $a \sin \beta$ reverses both the sequence of tetrahedral chains and the octahedral strip direction, giving $Q-P$. Table I gives the effect of symmetry operations on all the orientations of an I -beam; the information in the table matches Table A1 of Law and Whittaker (1980) in which the letters O and S (complete rotations) correspond to P and Q (different partial rotations).

The effect of symmetry operations on the I -beams can be used to derive the space groups of possible arrangements as illustrated for complete rotations in Table A2 of Law and Whittaker (1980). Selected arrangements of I -beams derived here are shown with their full space group symmetry (Tables II, III).

For the purpose of deriving space groups, P and Q represent distinct tetrahedral chains such that an I -beam containing P and Q chains is affected by symmetry operations in the ways shown in Table I. If the requirements of this table are met, some distortion of the tetrahedra in the P and Q chains and of the octahedra is permitted by the model, and it is in this respect that the model differs fundamentally from that of Thompson (1970). Some kind of distortion of the tetrahedra and the outermost regular M cation octahedra ($M1$ in pyroxene, $M2$ in amphibole) is associated with the adjustment of the structure where the 'parity rule' is violated (Papike and Ross, 1970; Sueno *et al.*, 1976). In principle, therefore, the present model has a mechanism by which parity violations can be accommodated.

Derivation of possible stacking arrangements. The possible stacking arrangements are described for the amphibole structure in which the I -beams have a mirror plane perpendicular to the b axis. The space groups for the corresponding arrangements in pyroxene can be derived by substituting a c -glide plane perpendicular to b .

TABLE I. Effect of symmetry operations on I-beams

Operation:	180° rotation about			Reflection perpendicular to		
	<i>asinb</i>	<i>b</i>	<i>c</i>	<i>asinb</i>	<i>b</i>	<i>c</i>
P+Q becomes	P-Q	Q+P	Q-P	Q-P	P+Q	P-Q
P-Q becomes	P+Q	Q-P	Q+P	Q+P	P-Q	P+Q
Q+P becomes	Q-P	P+Q	P-Q	P-Q	Q+P	Q-P
Q-P becomes	Q+P	P-Q	P+Q	P+Q	Q-P	Q+P
P+P becomes	P-P	P+P	P-P	P-P	P+P	P-P
P-P becomes	P+P	P-P	P+P	P+P	P-P	P+P

TABLE II. Model (1) Packing of I-beams with a single-layer a repeat

Model (1): All I-beams in a stack along *a* or *asinb* identically orientated.

(1)(i) Adjacent stacks similarly orientated
 $\begin{array}{l} \text{---} \text{---} \text{---} \text{---} \text{---} \text{---} \text{---} \text{---} \\ \text{---} \text{---} \text{---} \text{---} \text{---} \text{---} \text{---} \text{---} \end{array}$
 $\begin{array}{l} \cdot \text{P} + \text{Q} \cdot \text{P} + \text{Q} \cdot \text{P} + \text{Q} \cdot \\ + \text{Q} \cdot \text{P} + \text{Q} \cdot \text{P} + \text{Q} \cdot \text{P} + \end{array}$ C_m (amphibole)
 C_c (pyroxene)

(1)(ii) Adjacent stacks with oppositely directed octahedral strips
 $\begin{array}{l} \text{---} \text{---} \text{---} \text{---} \text{---} \text{---} \text{---} \text{---} \\ \text{---} \text{---} \text{---} \text{---} \text{---} \text{---} \text{---} \text{---} \end{array}$
 $\begin{array}{l} \cdot \text{P} + \text{Q} \cdot \text{P} + \text{Q} \cdot \text{P} + \text{Q} \cdot \\ - \text{Q} \cdot \text{P} - \text{Q} \cdot \text{P} - \text{Q} \cdot \text{P} - \end{array}$ $P2_1/m$ (amphibole)
 $P2_1/c$ (pyroxene)

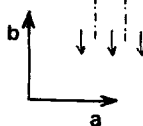
(1)(iii) Adjacent stacks with order of tetrahedral strips reversed
 $\begin{array}{l} \text{---} \text{---} \text{---} \text{---} \text{---} \text{---} \text{---} \text{---} \\ \text{---} \text{---} \text{---} \text{---} \text{---} \text{---} \text{---} \text{---} \end{array}$
 $\begin{array}{l} \cdot \text{P} + \text{Q} \cdot \text{P} + \text{Q} \cdot \text{P} + \text{Q} \cdot \\ + \text{P} \cdot \text{Q} + \text{P} \cdot \text{Q} + \text{P} \cdot \text{Q} + \\ \text{---} \text{---} \text{---} \text{---} \text{---} \text{---} \text{---} \text{---} \\ \text{---} \text{---} \text{---} \text{---} \text{---} \text{---} \text{---} \text{---} \end{array}$
 $\begin{array}{l} \cdot \text{P} + \text{Q} \cdot \text{P} + \text{Q} \cdot \text{P} + \text{Q} \cdot \\ + \text{P} \cdot \text{Q} + \text{P} \cdot \text{Q} + \text{P} \cdot \text{Q} + \end{array}$ $P2_1/m$ (amphibole)
 $P2_1/c$ (pyroxene)

(1)(iv) Adjacent stacks with both order of tetrahedral strips and octahedral strip direction reversed
 $\begin{array}{l} \text{---} \text{---} \text{---} \text{---} \text{---} \text{---} \text{---} \text{---} \\ \text{---} \text{---} \text{---} \text{---} \text{---} \text{---} \text{---} \text{---} \end{array}$
 $\begin{array}{l} \cdot \text{P} + \text{Q} \cdot \text{P} + \text{Q} \cdot \text{P} + \text{Q} \cdot \\ - \text{P} \cdot \text{Q} - \text{P} \cdot \text{Q} - \text{P} \cdot \text{Q} - \\ \text{---} \text{---} \text{---} \text{---} \text{---} \text{---} \text{---} \text{---} \\ \text{---} \text{---} \text{---} \text{---} \text{---} \text{---} \text{---} \text{---} \end{array}$
 $\begin{array}{l} \cdot \text{P} + \text{Q} \cdot \text{P} + \text{Q} \cdot \text{P} + \text{Q} \cdot \\ - \text{P} \cdot \text{Q} - \text{P} \cdot \text{Q} - \text{P} \cdot \text{Q} - \end{array}$ $Pm2_1$ (amphibole)
 $Pbc2_1$ (pyroxene)

Model (1) with all tetrahedral strips equivalent (P=Q)

(1)(v) $\begin{array}{l} \text{---} \text{---} \text{---} \text{---} \text{---} \text{---} \text{---} \text{---} \\ \text{---} \text{---} \text{---} \text{---} \text{---} \text{---} \text{---} \text{---} \end{array}$
 $\begin{array}{l} \cdot \text{P} + \text{P} \cdot \text{P} + \text{P} \cdot \text{P} + \text{P} \cdot \\ + \text{P} \cdot \text{P} + \text{P} \cdot \text{P} + \text{P} \cdot \text{P} + \\ \text{---} \text{---} \text{---} \text{---} \text{---} \text{---} \text{---} \text{---} \\ \text{---} \text{---} \text{---} \text{---} \text{---} \text{---} \text{---} \text{---} \end{array}$ $C2/m$ (amphibole)
 $C2/c$ (pyroxene)

(1)(vi) $\begin{array}{l} \text{---} \text{---} \text{---} \text{---} \text{---} \text{---} \text{---} \text{---} \\ \text{---} \text{---} \text{---} \text{---} \text{---} \text{---} \text{---} \text{---} \end{array}$
 $\begin{array}{l} \cdot \text{P} + \text{P} \cdot \text{P} + \text{P} \cdot \text{P} + \text{P} \cdot \\ - \text{P} \cdot \text{P} - \text{P} \cdot \text{P} - \text{P} \cdot \text{P} - \\ \text{---} \text{---} \text{---} \text{---} \text{---} \text{---} \text{---} \text{---} \\ \text{---} \text{---} \text{---} \text{---} \text{---} \text{---} \text{---} \text{---} \end{array}$ Pm (amphibole)
 Pbc (pyroxene)



The symmetry operators of the amphibole space group are marked on selected stacking diagrams.

TABLE III. Models (2)-(4) Packing of I-beams with a two-layer a repeat

<p>Model (2): Alternate I-beams in a stack have their octahedral strips oppositely directed.</p>		<p>Model (3): Alternate I-beams in a stack have the order of the tetrahedral strips reversed.</p>	
<p>(2)(i) Adjacent stacks similarly orientated</p> <p>. P + Q . P - Q . P + Q . - Q . P + Q . P - Q . P + Q . . P + Q . P - Q . P + Q . - Q . P + Q . P - Q . P + Q . . P + Q . P - Q . P + Q .</p> <p>$F2_{1ma}$ (amphibole) $F2_{1oa}$ (pyroxene) $2h+k=4n$ for $hk0$ reflections</p>	<p>(3)(i) Adjacent stacks similarly orientated</p> <p>. P + Q . Q + P . P + Q . + P . P + Q . Q + P . P + . P + Q . Q + P . P + Q .</p> <p>$F2_1/m$ (amphibole) $F2_1/o$ (pyroxene) $2h+k=4n$ for $hk0$ reflections</p>		
<p>(2)(ii) Adjacent stacks with oppositely directed octahedral strips</p> <p>. P + Q . P - Q . P + Q . + Q . P - Q . P + Q . P -</p> <p>Equivalent to (2)(i)</p>	<p>(3)(ii) Adjacent stacks with oppositely directed octahedral strips</p> <p>. P + Q . Q + P . P + Q . - P . P - Q . Q - P . P -</p> <p>$P2m2_1$ (amphibole) $Pbc2_1$ (pyroxene) $2h+k=4n$ for $hk0$ reflections</p>		
<p>(2)(iii) Adjacent stacks with order of tetrahedral strips reversed</p> <p>. P + Q . P - Q . P + Q . - P . Q + P . P - Q . Q + . P + Q . P - Q . P + Q . - P . Q + P . P - Q . Q + . P + Q . P - Q . P + Q .</p> <p>$P2ma$ (amphibole) $P2ca$ (pyroxene)</p>	<p>(3)(iii) Adjacent stacks with order of tetrahedral strips reversed</p> <p>. P + Q . Q + P . P + Q . + Q . Q + P . P + Q . Q +</p> <p>Equivalent to (3)(i)</p>		
<p>(2)(iv) Adjacent stacks with both order of tetrahedral strips and octahedral strip direction reversed</p> <p>. P + Q . P - Q . P + Q . + P . Q - P . Q + P . Q -</p> <p>Equivalent to (2)(iii)</p>	<p>(3)(iv) Adjacent stacks with both order of tetrahedral strips and octahedral strip direction reversed</p> <p>. P + Q . Q + P . P + Q . - Q . Q - P . P - Q . Q -</p> <p>Equivalent to (3)(ii)</p>		
<p>Model (4): Alternate I-beams in a stack have both the order of the tetrahedral strips reversed and the octahedral strips oppositely directed</p>		<p>Models (2) and (4) with all tetrahedral strips equivalent (P=Q)</p>	
<p>(4)(i) Adjacent stacks similarly orientated</p> <p>. P + Q . Q - P . P + Q . - P . P + Q . Q - P . P +</p> <p>$P2m2_1$ (amphibole) $Pbc2_1$ (pyroxene) $2h+k=4n$ for $hk0$ reflections</p>	<p>(2)(v)</p> <p>. P + P . P - P . P + P . - P . P + P . P - P . P + . P + P . P - P . P + P . - P . P + P . P - P . P +</p> <p>$P2ma$ (amphibole) $P2ca$ (pyroxene) $2h+k=4n$ for $hk0$ reflections</p>		
<p>(4)(ii) Adjacent stacks with oppositely directed octahedral strips</p> <p>. P + Q . Q - P . P + Q . + P . P - Q . Q + P . P -</p> <p>$F2_1/m$ (amphibole) $F2_1/o$ (pyroxene) $\beta = 90^\circ$ $2h+k=4n$ for $hk0$ reflections</p>	<p>(4)(iii) Adjacent stacks with order of tetrahedral strips reversed</p> <p>. P + Q . Q - P . P + Q . - Q . Q + P . P - Q . Q +</p> <p>Equivalent to (4)(ii)</p>		
<p>(4)(iv) Adjacent stacks with both order of tetrahedral strips and octahedral strip direction reversed</p> <p>. P + Q . Q - P . P + Q . + Q . Q - P . P + Q . Q -</p> <p>Equivalent to (4)(i)</p>			

The symmetry operators of the amphibole space group are marked on selected stacking diagrams.

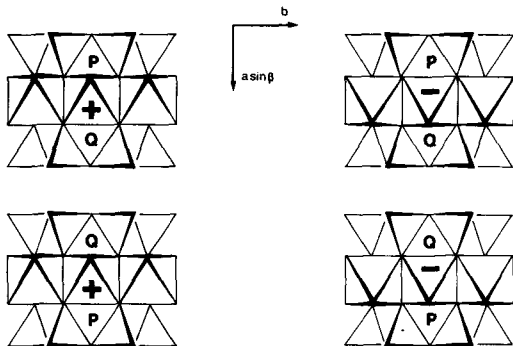


FIG. 5. Different orientations of an *I*-beam represented as $P+Q$, $P-Q$, $Q+P$, and $Q-P$ in the notation adopted here. P and Q denote differing tetrahedral rotations in the two chains, and $+$ and $-$ the directions of the octahedral strip. The different orientations of the *I*-beam result from reversing the sequences along $a \sin \beta$ of the two kinds of tetrahedral chain (P and Q) and (or) reversing the direction of the octahedral strip.

We shall restrict ourselves throughout to model structures containing only one kind of *I*-beam. The identical *I*-beams may, however, take up different orientations (fig. 5) when they are packed together.

Because we are now considering a model with chains of partially rotated tetrahedra, the constraint on the stacking sequence imposed by the requirement of close-packed oxygen planes is no longer applicable. In Thompson's (1970) terms, the 'parity rule' may be violated; it is known that such parity violations can be accommodated in real structures (Papike and Ross, 1970; Papike *et al.*, 1973) and are accompanied by distortion of the tetrahedra in the chains (Veblen and Burnham, 1978), and of the cation polyhedra at the edges of the *I*-beam (Sueno *et al.*, 1976). Since the present model permits such distortion there is no reason *a priori* to adhere to the parity rule, and it is therefore disregarded in the discussion which follows.

Consider first a model (1) in which all the *I*-beams in a stack along the *a* axis are identically orientated, i.e. $.P+Q.P+Q.P+Q$. The adjacent stack may be (i) similarly orientated, (ii) have the octahedral strip oppositely directed, (iii) have the order of the tetrahedral chains reversed, or (iv) have both the octahedral strip direction and the order of the tetrahedral chains reversed. These four arrangements and their space groups are shown in Table II together with the two special cases, (v) and (vi), which arise when the tetrahedra in the two chains of the *I*-beam are identically rotated. Models (1) (i)–(vi) all have one *I*-beam per repeat unit in the *a* direction, i.e. $a \sim 9 \text{ \AA}$.

The structures derived in Table II already include

three of the four known amphibole structure types. In order to account for orthoamphibole, we must extend the model to include arrangements with two *I*-beams per repeat unit in the *a* direction i.e. $a \sim 18 \text{ \AA}$. This can be done by allowing the stacks in the *a* direction to have alternating sequences of *I*-beams in different orientations, for which there are three possibilities:

- (2) Alternate *I*-beams have their octahedral strips oppositely directed, i.e.
 $.P+Q.P-Q.P+Q$.
- (3) Alternate *I*-beams have the order of the tetrahedral strips reversed, i.e.
 $.P+Q.Q+P.P+Q$.
- (4) Alternate *I*-beams have both the order of the tetrahedral strips reversed and the octahedral strips oppositely directed, i.e.
 $.P+Q.Q-P.P+Q$.

In each case, the second stack may be related to the first in the four ways (i)–(iv) described for model (1), giving in principle 12 possibilities for models (2)–(4), which are detailed in Table III.

Equivalences reduce the number of topologically distinct possibilities to six. The way in which these equivalences arise can be seen, for example, in model (2), in which the first stack has the sequence $.P+Q.P-Q.P+Q$. Reversing the octahedral strip direction in the second stack [model (2) (ii)] gives $.P-Q.P+Q.P-Q$, which is equivalent to leaving the orientation unchanged [model (2) (i)]. In the same way, in model (3), the first stack has $.P+Q.Q+P.P+Q$, and reversing the order of the tetrahedral chains [model (3) (iii)] gives $.Q+P.P+Q.Q+P$, which is also equivalent to leaving the orientation unchanged [model (3) (i)].

A number of the possibilities in Table III have non-space group symmetry. For example, in (2) (i), if we consider the projection down the *c*-axis, we find the point $\frac{1}{2}, \frac{1}{2}$ has exactly the same environment as the origin 0,0. This extra symmetry gives rise to an additional reflection condition $2h+k=4n$ for the $hk0$ reflections.

Successive tetrahedral chains in the *a* direction are displaced relative to each other by an amount which depends principally on the size of the $M4$ cation and the $O5-O6$ interchain contacts (Whittaker, 1960*a, b*). The direction of this displacement is controlled by the direction of the octahedral strip. The postulated structures with orthorhombic symmetry in Tables II and III all contain equal numbers of $+$ and $-$ octahedral strips in the *a* repeat as they must if β is to be 90° . Monoclinic structures such as (3) (i) (Table III) have all their octahedral strips similarly directed so that $\beta \neq 90^\circ$. Structure (4) (ii) (Table III) is exceptional in having monoclinic symmetry with $\beta = 90^\circ$, as the repeat

unit contains equal numbers of + and - octahedral chains.

When we consider the special case in which the tetrahedral chains are all similarly rotated, i.e. $P=Q$, model (3) reduces to model (1) with one *I*-beam in the *a* repeat; (3) (i) becomes the same as (1) (v), (3) (ii) the same as (1) (vi). Similarly, model (4) becomes the same as model (2) and (2) (iii) the same as (2) (i). It thus turns out that there is only one possible arrangement with two *I*-beams in the *a* repeat, for a structure with only one kind of tetrahedral chain, and this is shown as (2) (v) in Table III. This arrangement has the same space group, *Pnma*, as orthoamphibole (2) (iii) in Table III) but has the additional non-space group symmetry giving the reflection condition $2h+k=4n$ for *hk0* reflections.

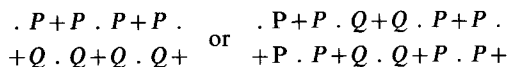
Comparison with other sets of structural models. The structural possibilities described by Law and Whittaker (1980) are derived for close-packed oxygen planes, i.e. for fully rotated tetrahedral chains, Thompson's (1970) treatment emphasizes the sense of the chain rotations but his 'parity rule' amounts to the assumption that oxygen packing controls the possible structure types.

The structural models described in Tables II and III can be related to those of Thompson (1970) and Law and Whittaker (1980) if the letters *P* and *Q* are taken to represent *O* and *S* rotations.

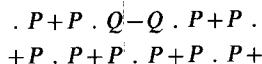
The following structures obey the 'parity rule' and match structure types listed by Thompson (1970) and by Law and Whittaker (1980): (1) (ii) $P2_1mn$, (1) (iii) $P2_1/m$, (1) (v) $C2/m$ and (4) (ii) $P2_1/m$ ($\beta = 90^\circ$) (Tables II and III). Structure (1) (v) with space group $C2/m$ corresponds to two possibilities listed by Thompson (1970) and by Law and Whittaker (1980), one with all *O* and one with all *S* rotations. The possible structure with $P2/m$ symmetry and one *I*-beam in the *a* repeat (Thompson, 1970; Law and Whittaker, 1980) does not arise in the approach adopted here as it contains two different kinds of *I*-beam, *O+O* and *S-S*.

All the other postulated structure types in Tables II and III violate the 'parity rule' and therefore lie outside the schemes of Thompson (1970) and Law and Whittaker (1980).

If the present model were to encompass all the possibilities listed by Law and Whittaker (1980) plus those violating the 'parity rule', it would need to be extended still further. The constraint that the structure must contain only one type of *I*-beam would have to be relaxed. If we took two kinds of tetrahedral strip present in equal numbers, this would allow structures like



which contain two or three different kinds of *I*-beam. To get the full range of possibilities, we should also have to take into account models such as



which contain two types of tetrahedral strip in the ratio 3:1.

Comparison with real pyribole structure types. We have derived possible structure types with one- and two-layer *a* repeats for pyriboles containing only one kind of *I*-beam. There are ten such possibilities if the *I*-beam contains two different tetrahedral chains (*P* and *Q*) and three for an *I*-beam with equivalent tetrahedral chains (i.e. $P=Q$). These thirteen models encompass the four well-established structure types for the pyriboles.

It is instructive to look for features which the known structure types have in common. The tetrahedral chains form layers parallel to (100) and, in all the four known structure types, these layers contain only one kind of tetrahedral chain. In clino- and proto-pyribole, this is because only one kind of tetrahedral chain is present. But in low clino- and ortho-pyribole, the structure has two kinds of tetrahedral layer, each containing only one kind of tetrahedral chain. In contrast, structures such as (1) (i) (Table II), which have only one kind of tetrahedral layer made up of two kinds of tetrahedral chain, are not found in nature. (Chesterite is exceptional in having both double and triple chains in its tetrahedral layer. According to Veblen and Burnham (1978), the tetrahedra at the edges of the multiple chains are rotated and distorted to a similar extent in each layer).

If, in deriving possible *I*-beam stacking arrangements, we impose the further restriction that tetrahedral layers may not contain two kinds of tetrahedral chain, we reduce the total number of possibilities from thirteen to the six shown in Table IV, without losing any of the known structure types.

Model (2) (v) is the result obtained when the tetrahedral chains of orthopyribole [model (2) (iii)] become identical. The space group is unaltered but the additional non-space group symmetry gives the reflection condition $2h+k=4n$ for *hk0* reflections. This additional reflection condition has been reported for the orthorhombic amphibole, holmquistite (Whittaker, 1969), and more recently for the triple-chain pyribole, jimthompsonite (Veblen and Burnham, 1978). It is tempting but erroneous to infer from this that these structures are examples of model (2) (v) with identical tetrahedral chains. The intensities of the *hk0* reflections with $2h+k \neq 4n$ are entirely determined by differences between the *x* and *y* coordinates of the tetrahedral

chains. However, information on the differences between the tetrahedral chains is also contained in the general *hkl* reflections and full three-dimensional structure refinements show that the chains do differ from each other. The differences in *x* and *y* coordinates are so small that the intensities of *hk0* reflections with $2h+k \neq 4n$ are below the limit of detection (Iruteta and Whittaker, 1975; Veblen and Burnham, 1978). Model (2) (v) is thus approached but not actually realized. With increasing temperature, the silicate chains in orthopyroxene become more alike (Smyth, 1973; Sueno *et al.*, 1976) and this too suggests an approach towards model (2) (v).

Model (1) (iv) can be derived from the protopyribole structure [model (1) (vi)] by allowing it to have two kinds of tetrahedral layer. There are no reports of protopyriboles showing reflections violating the reflection condition for an *n*-glide perpendicular to the *c* axis. If the differences between the tetrahedral layers were sufficiently small, model (1) (iv) might escape detection. It is in fact excluded in a more comprehensive derivation of the structure types (in preparation).

TABLE IV. Model structures from Tables II and III which do not have tetrahedral layers containing two different kinds of tetrahedral chain

Model	Space group		
	Amphibole	Pyroxene	
(1) (iii)	$P2_1/m$	$P2_1/c$	low clinopyribole
(1) (v)	$C2/m$	$C2/c$	clinopyribole
(1) (vi)	$Pnmm$	$Pbcn$	protopyribole
(2) (iii)	$Pnma$	$Pbca$	orthopyribole
(2) (v)	$Pnma$	$Pbca$	'high orthopyribole'
	$2h+k = 4n$ for <i>hk0</i> reflections		
(1) (iv)	$Pnm2_1$	$Pbc2_1$	'low protopyribole'

The four known pyribole structure types are listed first. Models (1) and (2) have one and two *I*-beams respectively in the *a* repeat unit.

The possibilities listed in Table IV seem to represent a reasonable set of potential pyribole structure types. These six model pyriboles can be subdivided into two groups of three: those with two kinds of tetrahedral chain or layer and those with only one. Those with two kinds of tetrahedral chain or layer are considered to be low-temperature structures; those with only one kind of tetrahedral chain, high-temperature forms.

Several pyroxenes have been described with space groups not found in Table IV. The 'low orthopyroxene' with space group $P2_1ca$ reported

by Smyth (1974) and Harlow *et al.* (1979) corresponds to model (2) (i) (Table III) but lacks the non-space group symmetry. The structure should therefore contain two kinds of *I*-beam and four kinds of tetrahedral chain but a full structure determination has not yet been performed to confirm this.

Smyth (1971) described a protoenstatite with space group $P2_1cn$ which corresponds to model (1) (ii) (Table II) and should contain two distinct silicate chains in the tetrahedral layer. But refinement of the structure did not reveal any departure from $Pbcn$ symmetry, and all other refinements of protoenstatite (Smith, 1969; Sadanaga *et al.*, 1969) converged satisfactorily in space group $Pbcn$.

Lindemann (1961) gave details of $MgSiO_3$ with space group $P2_1/n$. This allows only one type of tetrahedral chain but this has two different SiO_4 tetrahedra. A subsequent paper (Lindemann and Wögerbauer, 1974) gives the space group of similar material as Pc or $P2/c$.

$C2$ has been reported as the space group of a spodumene (Graham, 1975) though structure refinement revealed no departure from $C2/c$ symmetry. Only one type of tetrahedral chain is permitted by $C2$ but again with two distinct tetrahedra.

$P2/n$ must now be accepted as the space group of the omphacites since Matsumoto *et al.* (1975) have shown that multiple diffraction caused the weak reflections which led to the adoption of space group $P2$ initially. Lowering the symmetry from $C2/c$ permits a greater degree of ordering of the octahedral cations; two different SiO_4 tetrahedra occur in the one type of chain permitted in space group $P2/n$.

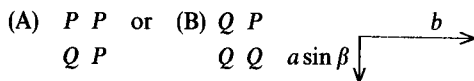
Doubts have been expressed over the existence of $P2_1ca$ low orthopyroxene (Sueno *et al.*, 1976; Veblen and Burnham, 1978), $P2_1cn$ protoenstatite (Smyth and Ito, 1977), $P2_1/n$ $MgSiO_3$ (Smith, 1969), and $C2$ spodumene (Graham, 1975) but none of these has been conclusively discredited. There is no doubt that omphacite has lower symmetry than $C2/c$. It is a limitation of the model for pyribole structure types described here that structures such as these lie outside its scope. A paper is in preparation which presents a more comprehensive derivation which includes the low symmetry pyroxenes.

Structural control of the I-beam packing. The six model biopyribole structures in Table IV have been derived using two rules: (a) that the structures may not contain more than one kind of *I*-beam, and (b) that a tetrahedral layer may not contain more than one kind of tetrahedral chain. The rules proposed here must have their origin in the nature of the crystal structure itself.

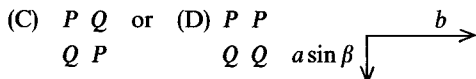
The second rule, that a tetrahedral layer must contain only one kind of tetrahedral chain, must

arise from the edgewise packing of the *I*-beams, since this is how the tetrahedral chains form layers parallel to (100). This packing is likely to be controlled either by the coordination of the outermost *M* cation (*M*2 in pyroxene, *M*4 in amphibole, *M*5 in jimthompsonite) which is linked to *O* atoms in four tetrahedral chains (three different *I*-beams), or by the edge-to-edge packing of the tetrahedral chains themselves.

The outermost *M* cation is linked to oxygen atoms in four tetrahedral chains, which must adjust their oxygen packing in some way to fit the awkward coordination polyhedron of the outer *M* site. In models (3) and (4), the outermost *M* cation is linked to three tetrahedral chains of one kind and one of the other, i.e.



It seems likely that in these cases the tetrahedral chains will be less able to take up departures from ideal oxygen packing than in models (1) and (2) in which the outermost *M* cation is linked to two tetrahedral chains of each kind, i.e.



This could explain why models (3) and (4) do not occur in nature but would not fully explain rule (b). *A priori* there is no reason why (C) and (D) should not be equally preferable, though only (D) is found.

The key to the origin of rule (b) must lie in the edge-to-edge packing of the tetrahedral chains into layers. If the tetrahedral layers were unconstrained by the linkage to the octahedral strips, they would adopt some ideal configuration in which the Si-O and O-O distances had optimum values. The linkage of the oxygen atoms to the *M* cations of the octahedral strips causes a departure from the idealized tetrahedral layer configuration. This departure from ideality may consist of (i) tetrahedral chain rotation, (ii) distortion of the tetrahedral chain by atomic displacements. In general, both will occur but one will predominate. We shall consider each in turn.

(i) For chains of rotated tetrahedra, the packing of oxygen atoms in the tetrahedral layer will be optimized if the rotations are equal in magnitude and in the senses indicated in fig. 6 for fully rotated tetrahedra. For this to be so, the tetrahedral chains must be related by 2_1 axes parallel to *b*. Since the amount of the rotation is determined by the sizes of the octahedra in the attached strips, these strips too must be related by the 2_1 axes and must therefore be similarly directed. This then makes adjacent

tetrahedral chains either both *O*- or both *S*-rotated. This is the result predicted by the first part of Thompson's 'parity rule', i.e. that if the tetrahedra are rotated in the same sense, the octahedral strips above and below the tetrahedral layer must be similarly directed. The need for the octahedral strips to be related by the 2_1 axes, because they control the tetrahedral rotation, explains why there is no instance of the second part of Thompson's 'parity rule', i.e. of oppositely directed octahedral strips with tetrahedral chains rotated in opposite senses.

(ii) For tetrahedral chains distorted by atomic displacements, the symmetry requirement is controlled by the atomic displacements in the *c* direction. The oxygen packing will be optimized if the changes in *z* coordinate are equal and in the *same* sense relative to the crystallographic axes in adjacent chains (fig. 7). This requires adjacent chains to be related by a glide plane parallel to (100) (*b* glide in pyroxene, *n* glide in amphibole).

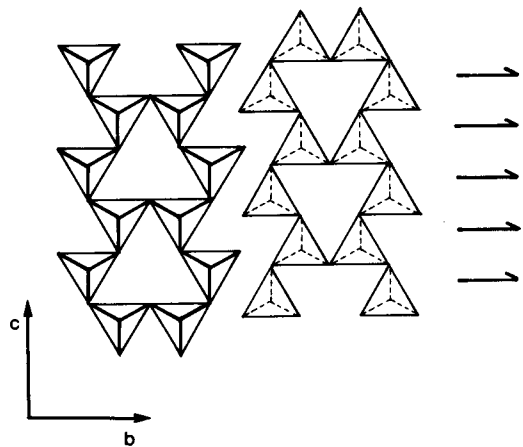
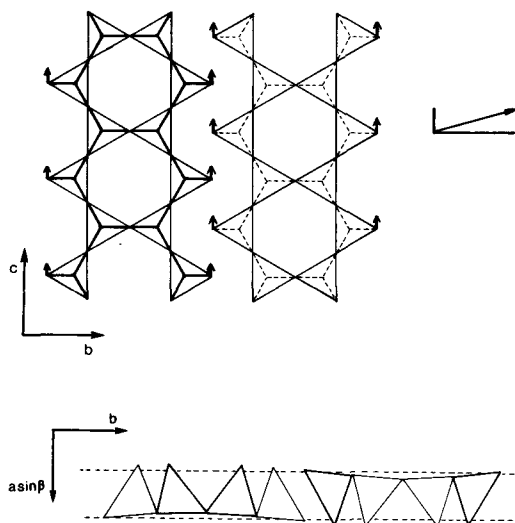


FIG. 6. Edge-to-edge packing of fully rotated tetrahedral chains in amphibole, showing that adjacent chains must be related by 2_1 axes for optimum atomic packing.

Atomic displacements in the *b* direction must take the outer atoms of the chain towards or away from its centre if the chain is to retain its symmetry (mirror plane in amphibole, *c* glide plane in pyroxene). These displacements in the *b* direction must be equal in adjacent chains otherwise the electrostatic interactions will tend to make them so. Such displacements are consistent with either 2_1 axes or a glide plane in the tetrahedral layer.

Atomic displacements in the *a* direction are the major contribution to the bending or warping of the chains. If we assume that departures of the oxygen atoms from some nearly close-packed (100) plane are to be minimized, adjacent chains must



FIGS. 7 and 8. FIG. 7 (*above*). Fully extended tetrahedral chains in amphibole. An atomic displacement along c (arrow) at the edge of the chain will distort the tetrahedra, shortening some oxygen-oxygen distances to the adjacent chain and lengthening others. To counteract this, the atomic displacements in the adjacent chain must be in the same direction and the chains are then related by an n -glide plane. FIG. 8 (*below*). Warping or bending of tetrahedral chains in amphibole. Adjacent chains must be equally bent in opposite senses if the departures of the oxygen atoms from a nearly close-packed (100) plane (dashed line) is to be minimized.

be bent equally but in opposite senses (fig. 8) and this would fit either 2_1 axes or a glide plane in the tetrahedral layer.

The atomic displacements are controlled mainly by the sharing of edges between the outer tetrahedra and the outer M octahedra and can have a substantial component in the c direction (Veblen and Burnham, 1978). If the atomic displacements in adjacent chains are to be equal, a glide plane is required in the tetrahedral layer and the octahedral strips must be related by this and therefore be oppositely directed. This corresponds to the parity violation in which tetrahedral chains with similar rotations are linked to oppositely directed octahedral strips. This type of parity violation occurs in ortho- and proto-pyribole whereas there is no example of the other type of violation, i.e. similarly directed octahedral strips on either side of a tetrahedral layer with alternate chains rotated in opposite senses.

It should be noted that the 2_1 axes and the glide plane in the two cases (i) and (ii) are incompatible except for fully extended, undistorted tetrahedral chains. In real structures, the oxygen packing must

therefore be optimized either for tetrahedral rotation at the expense of atomic displacements (giving 2_1 axes) or for atomic displacements at the expense of tetrahedral rotations (giving a glide plane).

But both cases (i) and (ii) require that only one kind of tetrahedral chain should be present in a tetrahedral layer. Rule (*b*) therefore results from the fundamental need to optimize the atomic packing in the tetrahedral layer.

The rule (*b*) that a tetrahedral layer may not contain two different kinds of tetrahedral chain is in fact more fundamental than the 'parity rule'. Rule (*b*) covers both the case of the 'parity rule' which is known to occur and the type of parity violation which is found in pyribole structures. It excludes the case of the parity rule of which no example is known, and it also excludes the type of parity violation which does not occur.

So powerful is rule (*b*) that it almost eclipses the requirement of rule (*a*) that the structure shall contain only one kind of I -beam. If we began by deriving the structural possibilities conforming to rule (*b*), we should obtain directly all the possibilities in Table IV without invoking rule (*a*) at all. However, we should then also obtain model structures with a two-layer a -repeat, which contain four kinds of tetrahedral layer. Rule (*a*) is needed to eliminate these but can be restated in the form: the structure may contain only two different kinds of tetrahedral layer.

Can we explain why there should be only two kinds of tetrahedral layer? What in the pyribole structure might give rise to two kinds of tetrahedral layer? The distortion of the tetrahedral layers (the combined effect of chain rotation and atomic displacements) results from the links to the octahedral strips on either side. If the tetrahedral chains lie between similarly directed octahedral strips ($-$ chains), the distortion is principally chain rotation as shown by fig. 14¹ of Veblen and Burnham (1978), and the tetrahedral layer should contain 2_1 axes but no glide plane.¹ For tetrahedral chains between oppositely directed octahedral strips (\times -chains), the distortion includes appreciable atomic displacements (fig. 12 of Veblen and Burnham, 1978) of the kind shown in fig. 13 of Veblen and Burnham (1978), and the tetrahedral layer has a glide plane but no 2_1 axes.

Could it be that the two kinds of tetrahedral layer are defined by the relative direction of the octahedral strips on either side of them? The structure types would then have $-$ chains between octahedral strips similarly directed and \times -chains

¹ Note that figs. 12 and 14 of Veblen and Burnham are transposed; the fig. 12 caption on p. 1068 refers to the figure on p. 1069 above the fig. 14 caption and vice versa.

between oppositely directed strips. If the type of chain were determined by octahedral strip directions in this way, 'low protopyribole' would be eliminated since it would consist of all \times -chains which would have to be identical as in protopyribole. 'High orthopyribole' would also be eliminated since it has both $\cdot\cdot$ - and \times -chains which must differ. Unfortunately this assumption would also eliminate low clinopyribole as containing $\cdot\cdot$ -chains only which would have to be identical. There are too many examples of this structure type (particularly of pigeonites) for its exclusion to be reasonable. The model has clearly been pressed a little too far. None the less, it emphasizes Thompson's (1970) point that the main structure types contain a $\cdot\cdot\cdot$ chain sequence only (clinopyribole), a $\times \times \times$ sequence only (proto-) or an alternating sequence $\cdot \times \cdot$ (ortho-).

We have been led here into the apparently circular argument that the octahedral sequence controls the distortion of the tetrahedral layer, which controls the octahedral sequence. However, what is really being described is the way in which the regular stacking sequence is communicated through the structure.

The possible structure types result from the symmetry requirements for optimum packing of the tetrahedral chains into layers. The coordination of the octahedral cations, particularly of the outermost cation in the strip, determines which structure type will be obtained for a given composition.

Phase transitions in the pyriboles. The relative stability of the main structure types will be a function of the strains in the atomic arrangement of each. We may conjecture that there are two main sources of strain in the pyribole structure. The silicate chains distorted by atomic displacements (\times -chains) are likely to be highly strained and the number of such chains in the structure increases in the sequence

clino- < ortho- < proto-

There will also be strain associated with the outermost M cation polyhedra depending on the cation radius. The sizes of the $M4$ polyhedra in amphibole and $M2$ in pyroxene increase in the sequence

proto- < ortho- < clino-

The calcic and sodic pyriboles have large cations (Ca, Na) in the outermost M sites and should adopt the clino-structure type as that of least strain on both counts.

The ferromagnesian pyriboles have smaller cations (Fe^{2+} , Mg) in the outermost M sites and the strain associated with these should increase in the sequence

proto- < ortho- < clino-

The strain associated with the \times -chains, however, increases in the opposite sequence, i.e.

clino- < ortho- < proto-

It seems reasonable to suppose that orthopyribole is the most likely low-temperature phase, being a compromise between these opposing trends. The high-temperature phase will depend on which of the strains is larger. For small cations, the strain at the outer M site is likely to predominate and the high-temperature phase should be proto-. Clino- would be the expected high-temperature phase for larger outer M cations, when the strain from the \times -chains should predominate.

On the MgSiO_3 - $\text{CaMgSi}_2\text{O}_6$ phase diagram, one would therefore expect orthopyroxene as the low temperature structure for MgSiO_3 , with protopyroxene as the high-temperature structure. For $\text{CaMgSi}_2\text{O}_6$ the clinopyroxene structure should be stable up to the liquidus. Between enstatite (MgSiO_3) and diopside ($\text{CaMgSi}_2\text{O}_6$) there is a Mg-rich orthopyroxene-Ca-rich clinopyroxene solvus because of the disparity in the sizes of the $M2$ cations.

As already suggested (Papike *et al.*, 1973), low clinopyroxene may provide a means of relieving strain at the $M2$ site in clinopyroxene without its undergoing the difficult reconstructive transformation to orthopyroxene. With increasing temperature and increasing $M2$ cation size (increasing Ca content), this relief of strain apparently lowers the free energy sufficiently to give the low clinopyroxene structure a stability field as pigeonite. This could coexist with either a clinopyroxene richer in Ca (diopside) or an orthopyroxene richer in Mg, as is shown on the phase diagram of Longhi and Boudreau (1980).

At temperatures where protoenstatite is the stable phase of MgSiO_3 , the insertion of a little Ca stabilizes the orthopyroxene structure with its slightly larger $M2$ sites. The narrow protoenstatite-orthoenstatite solvus so produced does not overlap the orthoenstatite-pigeonite solvus with the result that pigeonite cannot coexist with protoenstatite.

Of the phases listed in Table IV, only 'low protopyroxene' and 'high orthopyroxene' do not appear on the phase diagram of Longhi and Boudreau (1980). 'High orthopyribole' almost certainly cannot exist. The orthorhombic structure has alternate tetrahedral layers with 2_1 axes and with glide planes, which must be identical in the high-temperature form. But these two symmetry operators are only compatible with each other for fully extended undistorted tetrahedral chains, which are unlikely to be reached at a temperature below the transformation to proto- or clino-. 'High orthopyribole' can only be imagined as an extrapolation

of the changes in the orthorhombic structure with increasing temperature described for orthoenstatite by Smyth (1973), and for orthoferrosilite by Sueno *et al.*, (1976).

Conclusion. The rule that a pyribole structure may contain two types of tetrahedral layer but no tetrahedral layer may contain two types of tetrahedral chain, leads to a reasonable set of model pyribole structures, including all the well-established types. This rule is more fundamental than the 'parity' rule and has its origin in the optimization of the edge-to-edge packing of the tetrahedral chains into layers. The model structures derived are consistent with the crystal chemistry and phase relations of the pyriboles.

The treatment adopted here leads naturally to the \cdot - and \times -chains notation used by Veblen and Burnham (1978), following J. B. Thompson's unpublished work. It is reassuring that such similar conclusions may be reached by quite different approaches.

Acknowledgement. The author is grateful to Mr P. G. Embrey and Dr D. R. Veblen for their carefully considered criticism and comments.

REFERENCES

- Graham, J. (1975). Some notes on α -spodumene. *Am. Mineral.* **60**, 919-23 [MA 76-1919].
- Harlow, G. E., Nehru, C. E., Prinz, M., Taylor, C. J., and Keil, K. (1979). Pyroxenes in Serra de Magé: cooling history in comparison with Moama and Moore County. *Earth Planet. Sci. Lett.* **43**, 173-81.
- Irusteta, M. C., and Whittaker, E. J. W. (1975). A three-dimensional refinement of the structure of holmquistite. *Acta Crystallogr.* **B31**, 145-50 [MA 76-201].
- Law, A. D., and Whittaker, E. J. W. (1980). Rotated and extended model structures in amphiboles and pyroxenes. *Mineral. Mag.* **43**, 565-74 [MA 80-1289].
- Lindemann, W. (1961). Gitterkonstanten, Raumgruppe und Parameter des γ -MgSiO₃. *Naturwiss.* **48**, 428-9.
- and Wögerbauer, R. (1974). Gitterkonstanten und Raumgruppe für Protoenstatit (MgSiO₃). *Ibid.* **61**, 500.
- Longhi, J., and Boudreau, A. E. (1980). The orthoenstatite liquidus field in the system forsterite-diopside-silica at one atmosphere. *Am. Mineral.* **65**, 563-73.
- Matsumoto, T., Tokonami, M., and Morimoto, N. (1975). The crystal structure of omphacite. *Ibid.* **60**, 634-41 [MA 76-198].
- Pannhorst, W. (1979). Structural relationships between pyroxenes. *Neues Jahrb. Mineral. Abh.* **135**, 1-17 [MA 79-3367].
- Papike, J. J., Prewitt, C. T., Sueno, S., and Cameron, M. (1973). Pyroxenes: comparisons of real and ideal structural topologies. *Z. Kristallogr.* **138**, 254-73 [MA 74-902].
- and Ross, M. (1970). Gedrites: crystal structures and intracrystalline cation distributions. *Am. Mineral.* **55**, 1945-72 [MA 71-1754].
- Sadanaga, R., Okamura, F. P., and Takeda, H. (1969). X-ray study of the phase transformations of enstatite. *Mineral. J.* **6**, 110-30 [MA 72-1806].
- Smith, J. V. (1969). Crystal structure and stability of the MgSiO₃ polymorphs: physical properties and phase relations of Mg, Fe pyroxenes. *Mineral. Soc. Am. Spec. Pap.* **2**, 3-29 [MA 70-2098].
- Smyth, J. R. (1971). Protoenstatite: a crystal-structure refinement at 1100°C. *Z. Kristallogr.* **134**, 262-74 [MA 72-2753].
- (1973). An orthopyroxene structure up to 850°C. *Am. Mineral.* **58**, 636-48 [MA 74-154].
- (1974). Low orthopyroxene from a lunar deep crustal rock: a new pyroxene polymorph of space group $P2_1ca$. *Geophys. Res. Lett.* **1**, 27-9 [MA 75-2343].
- and Ito, J. (1977). The synthesis and crystal structure of a magnesium-lithium-scandium protopyroxene. *Am. Mineral.* **62**, 1252-7 [MA 78-2704].
- Sueno, S., Cameron, M., and Prewitt, C. T. (1976). Orthoferrosilite: high-temperature crystal chemistry. *Ibid.* **61**, 38-53.
- Thompson, J. B. (1970). Geometrical possibilities for amphibole structures: model biopyriboles (abstract). *Ibid.* **55**, 292-3.
- (1978). Biopyriboles and polysomatic series. *Ibid.* **63**, 239-49 [MA 78-4032].
- Veblen, D. R., and Burnham, C. W. (1978). New biopyriboles from Chester, Vermont: II. The crystal chemistry of jimthompsonite, clinojimthompsonite, and chesterite, and the amphibole-mica reaction. *Ibid.* **63**, 1053-73 [MA 79-2107].
- Whittaker, E. J. W. (1960a). The crystal chemistry of the amphiboles. *Acta Crystallogr.* **13**, 291-8 [MA 15-96].
- (1960b). Relationships between the crystal chemistry of pyroxenes and amphiboles. *Ibid.* **13**, 741-2 [MA 15-96].
- (1969). The structure of the orthorhombic amphibole holmquistite. *Ibid.* **B25**, 394-7 [MA 71-1756].

[Manuscript received 3 June 1980;
revised 17 October 1980]